Bioorganic & Medicinal Chemistry xxx (xxxx) xxxx

Contents lists available at ScienceDirect

Bioorganic & Medicinal Chemistry

journal homepage: www.elsevier.com/locate/bmc

Synthesis and elaboration of *N*-methylpyrrolidone as an acetamide fragment substitute in bromodomain inhibition

J.P. Hilton-Proctor[a], O. Ilyichova[a], Z. Zheng[a], I.G. Jennings[a], R.W. Johnstone[b,c], J. Shortt[d,e], S.J. Mountford[a], M.J. Scanlon[a], P.E. Thompson[a,*]

[a] Medicinal Chemistry, Monash Institute of Pharmaceutical Science, Monash University, 381 Royal Parade, Parkville, Victoria, Australia
[b] Peter MacCallum Cancer Centre, 305 Grattan Street, Melbourne, Victoria, Australia
[c] The Sir Peter MacCallum Department of Oncology, University of Melbourne, Parkville, Victoria, Australia
[d] Blood Cancer Therapeutics Laboratory, School of Clinical Sciences at Monash Health, Monash University, 246 Clayton Road, Clayton, Victoria, Australia
[e] Monash Haematology, Monash Health, 246 Clayton Road, Clayton, Victoria, Australia

ARTICLE INFO

Keywords:
BRD4
Bromodomain
Acetyl-lysine
NMP
N-Methylpyrrolidone
Olinone
Fragment-based drug design

ABSTRACT

N-Methylpyrrolidone is a solvent molecule which has been shown to compete with acetyl-lysine-containing peptides for binding to bromodomains. From crystallographic studies, it has also been shown to closely mimic the acetamide binding motif in several bromodomains, but has not yet been directly pursued as a fragment in bromodomain inhibition. In this paper, we report the elaboration of *N*-methylpyrrolidone as a potential lead in fragment-based drug design. Firstly, *N*-methylpyrrolidone was functionalised to provide points for chemical elaboration. Then, the moiety was incorporated into analogues of the reported bromodomain inhibitor, Olinone. X-ray crystallography revealed that the modified analogues showed comparable binding affinity and structural mimicry to Olinone in the bromodomain binding site.

1. Introduction

Bromodomains are protein domains that are recognition elements for acetyl-lysine (K-ac) residues, and act as "readers" to regulate the cellular functions of bromodomain-containing proteins (BCPs). In total, 46 BCPs have been reported in humans that comprise 61 different bromodomains divided into 8 subfamilies. With established roles in transcriptional activation,[1] BCPs have been associated with a number of disease states relating to cancer,[2–4] viral diseases,[5–9] inflammation[10,11] and cardiovascular diseases.[12,13] Bromodomain inhibitors have therefore been identified as potential therapeutic agents[14–16] and numerous compounds are currently under clinical investigation.[17–21]

Bromodomains have a conserved three-dimensional structure consisting of a series of four α-helices (αZ, αA, αB, αC) linked by two interhelical loops (ZA, BC)[22] where the space between these loops creates the cavity where K-ac is recognised. This binding site has been effectively targeted by various bromodomain inhibitors, with the bromodomain and extra-terminal (BET) family of BCPs serving as the prototype for inhibitor design. Initially, the methyltriazolodiazepines (+)-JQ1[23] and I-BET762[11] were identified as K-ac mimetics among a host of other chemotypes. Since then, it has become a fruitful subject for fragment-based drug design (FBDD) approaches. Chung[24] and Bamborough[25] both described a FBDD approach that identified an array of low molecular weight compounds, including the 3,5-dimethylisoxazoles, which were also described by Hewings et al.[26] Virtual screening approaches using fragment substructures have also yielded K-ac mimetics.[27] Additionally, the alkylacetamide function of K-ac has been mimicked directly in the inhibitor Olinone,[28] which selectively targets the first bromodomain of BET proteins (Fig. 1).

The solvent, *N*-methylpyrrolidone (NMP) also interacts with the binding pocket of a range of bromodomains,[31] and was shown to be a mimetic of K-ac in crystallographic studies where it binds to the

Abbreviations: ATAD2, ATPase Family AAA Domain-containing Protein 2; BCP, Bromodomain-containing Protein; BET, Bromodomain and Extra-terminal; BRD#, Bromodomain-containing Protein #; BRD4 BD1, First Bromodomain of BRD4; CBP, Cyclic AMP Response Element Binding Protein Binding Protein; FBDD, Fragment-based Drug Design; FRET, Fluorescence Resonance Energy Transfer; GST, Glutathione *S*-transferase; K-ac, Acetyl-lysine; IRF-4, Interferon Regulatory Factor 4; LE, Ligand Efficiency; LPS, Lipopolysaccharide; NHA, Non-hydrogen Atom; NMP, *N*-Methylpyrrolidone; NMR, Nuclear Magnetic Resonance; PB1, Polybromo-1; PHIP, Pleckstrin Homology Domain Interacting Protein; RMS, Root Mean Square; SAR, Structure-Activity Relationship; SMARCA4, SWI/SNF Related Matrix Associated Actin Dependent Regulator of Chromatin Subfamily A Member 4; vdW, van der Waals

* Corresponding author.
E-mail address: philip.thompson@monash.edu (P.E. Thompson).

https://doi.org/10.1016/j.bmc.2019.115157
Received 14 August 2019; Received in revised form 7 October 2019; Accepted 8 October 2019

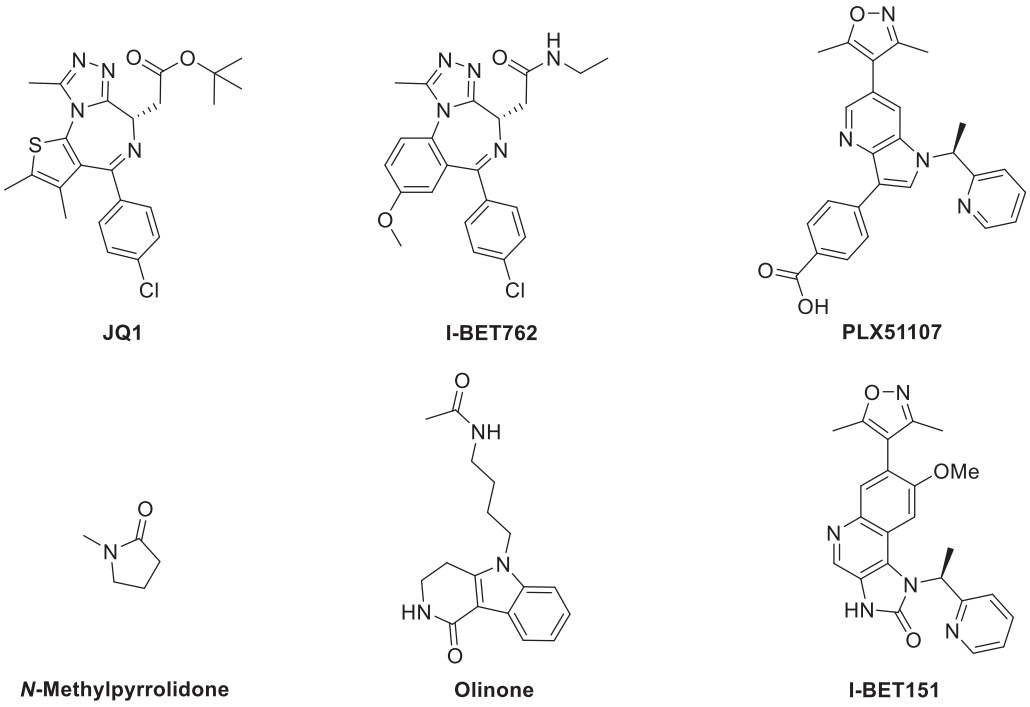

Figure 1. Reported bromodomain inhibitors and probes.[11,23,28–31.]

conserved areas of the bromodomain binding pocket in bromodomain-containing protein 1 (BRD1, PDB: 3RCW), BRD2 (PDB: 4A9F), ATPase family AAA domain-containing protein 2 (ATAD2, PDB: 4QSS), cyclic AMP response element binding protein binding protein (CBP, PDB: 3P1D), SWI/SNF related matrix associated actin dependent regulator of chromatin subfamily A member 4 (SMARCA4, PDB: 3UVD), polybromo-1, (PB1, PDB: 3MB4) and pleckstrin homology domain interacting protein (PHIP, PDB: 3MB3). NMP inhibits the binding of acetylated histone peptides to a range of BCPs at millimolar concentrations[32] while its affinity, despite being modest, was comparable to that of K-ac, giving it good ligand efficiency (LE) because of its low molecular weight.[31]

The pleiotropic bromodomain inhibition shown by NMP may be pharmacologically relevant and contribute to its anti-myeloma and immunomodulatory activity, showing hallmark reduction in transcription factors *c-Myc* and interferon regulatory factor 4 (IRF-4) in multiple myeloma models.[32] This activity has seen it advance into a phase I clinical trial for multiple myeloma (NCT02468687).[33] Additionally, NMP has been suggested as an anti-bone resorptive therapy in diseases such as osteoporosis where bromodomain inhibition mediates the prevention of osteoclast differentiation,[34] inhibits lipopolysaccharide (LPS)-induced inflammatory mediators[35] and reduces the effects of adipocyte accumulation.[36]

Despite the structural and functional evidence of NMP's bromodomain inhibitor mimicry, its use as a fragment in FBDD has not been reported. It was described as the inspiration behind other mimetic warheads such as the 3,5-dimethylisoxazole,[26,37] but while NMP has a high LE, additional functionalisation would be necessary to explore its potential in fragment elaboration. Here, we report our expansion of the NMP template with a range of functional groups and the subsequent elaboration by mimicry of Olinone as an exemplar of the broader approach to bromodomain inhibitor design. X-ray crystal structures of the NMP derivatives show the successful mimicry of the native acetamide binding pose.

2. Results and discussion

In crystal structures of NMP bound to different bromodomains, a conserved mode of binding is observed. The carbonyl moiety of NMP forms a hydrogen bond with the highly conserved asparagine residue, as well as a water-mediated hydrogen bond to a conserved tyrosine in the K-ac binding pocket, while the *N*-methyl substituent sits adjacent to the water-lined pocket. We posited that the 4-position of NMP would be a suitable point to elaborate the NMP structure (Supplementary Video S1).

2.1. Synthesis

We developed two series of NMP derivatives with functional groups from which to elaborate using two synthetic routes. The first series was derived from methyl 1-methyl-5-oxopyrrolidine-3-carboxylate **2** (Scheme 1). Dimethyl itaconate **1** was treated with methylamine and then cyclised *in situ* to give **2** in 91% yield as previously reported.[38,39] The ester **2** was then reduced to the alcohol **3** with excess sodium borohydride in 88% yield.[38] The final step was the conversion of the

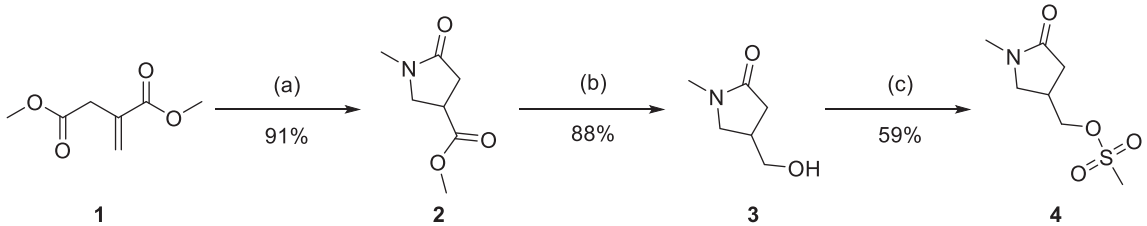

Scheme 1. Formation of **4**, a mesylate NMP derivative. (a): CH_3NH_2, MeOH, 0 °C → rt, o/n; (b): $NaBH_4$, EtOH; rt, o/n; (c): N_2, MsCl, DIPEA, CH_2Cl_2, 0 °C, 4 h.

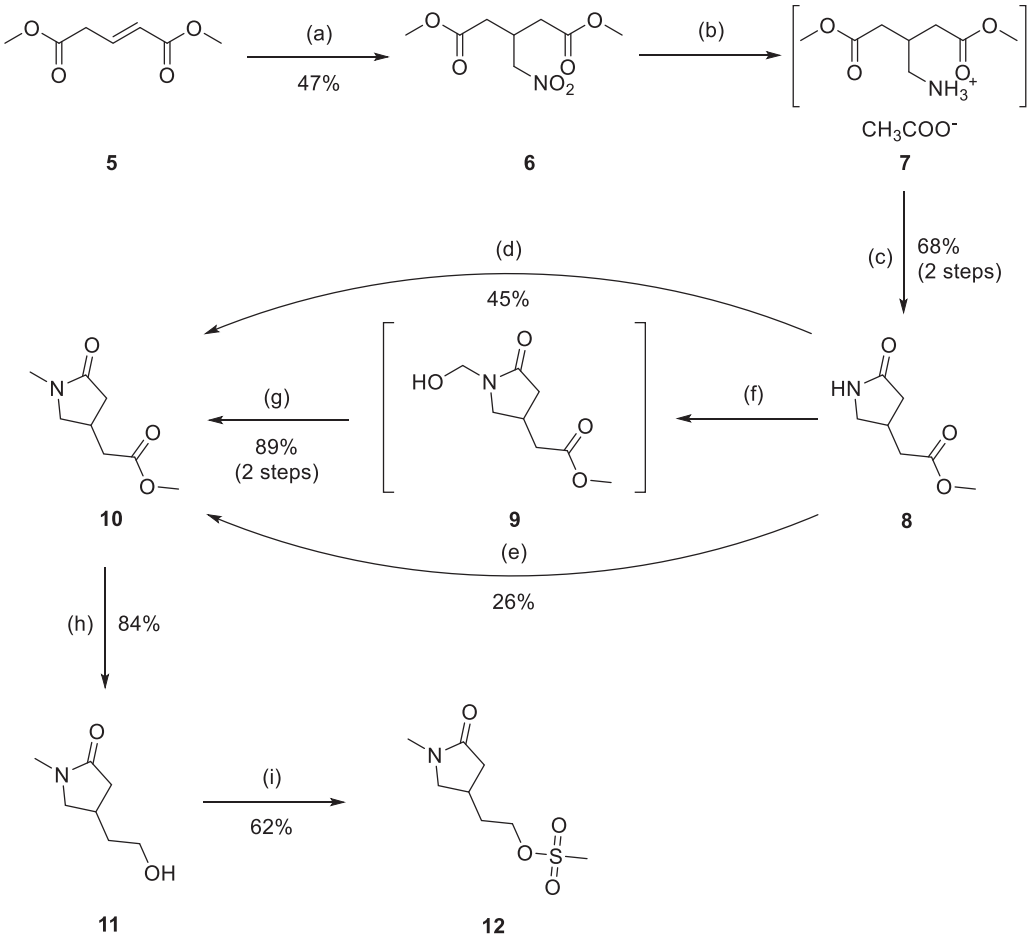

Scheme 2. Formation of **12**, a dimethylene NMP mesylate. (a): CH_3NO_2, 1,1,3,3-tetramethylguanidine, 42 h, rt; (b): H_2, Pd/C, CH_3COOH, 5 d, rt; (c): Et_3N, MeOH, o/n, reflux; (d): N_2, *t*-BuOK, MeI, THF, 6 h, 0 °C; (e): K_2CO_3, MeI, CH_3CN, 6 d, reflux; (f): Paraformaldehyde, K_2CO_3, acetone, H_2O, 4 h, rt; (g): Et_3SiH, CF_3COOH, $CHCl_3$, o/n, rt; (h): $NaBH_4$, EtOH; rt, o/n; (i): N_2, MsCl, DIPEA, CH_2Cl_2, 0 °C, 4 h.

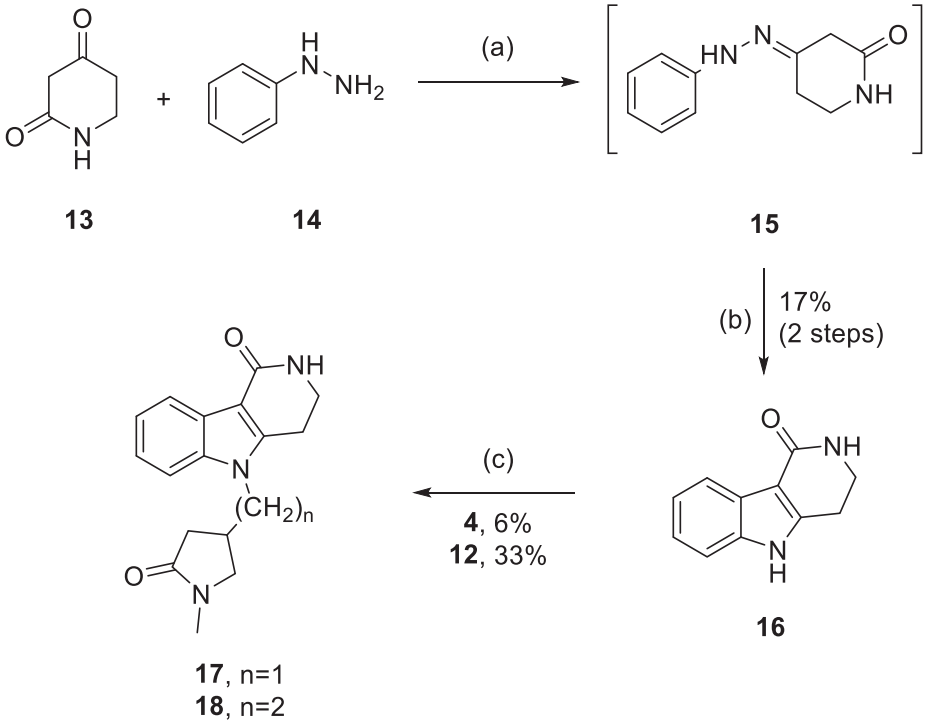

Scheme 3. Preparation of 2,3,4,5-tetrahydro-1*H*-pyrido[4,3-*b*]indol-1-one **16** and coupling to NMP derivatives **4** and **12**. (a): EtOH, rf, o/n; (b): 70% H_2SO_4, 0 °C, 4 h; (c): N_2, NaHMDS, DMF, –78 °C → 90 °C, o/n.

alcohol to a mesylate through the use of methanesulfonyl chloride and DIPEA under an inert atmosphere to give **4** in 59% yield.[40,41]

In the second series, compounds **10**, **11** and **12** were prepared as shown in Scheme 2. Dimethyl glutaconate **5** was treated with nitromethane and 1,1,3,3-tetramethylguanidine[42] to afford the nitroester **6** in 47% yield. The nitroester **6** was reduced to the amine **7** with the use of palladium on carbon under a hydrogen atmosphere with acetic acid as the solvent, which gave the amine **7** as an acetate salt. The amine **7** was refluxed in a mixture of methanol and triethylamine to neutralise the acetate salt and catalyse the cyclisation to form the lactam **8** in 68% yield over two steps.

The lactam derivative **8** was *N*-methylated by conversion to the hemiaminal intermediate **9** through treatment with paraformaldehyde and potassium carbonate, which was then reduced with triethylsilane and trifluoroacetic acid to give **10** in 89% yield across the two steps.[43] In contrast, yields for direct methylation with methyl iodide in the presence of a base were modest at best.[44–46] Finally, the reduction of the ester **10** to the alcohol **11** and subsequent conversion to the mesylate **12** were carried out using the same methods described for **3** and **4** in similar yields. Collectively, we have built a set of six analogues of NMP substituted at the 4-position. Each of these compounds, **2–4** and **10–12**, is amenable to further elaboration.

Olinone was originally reported by Gacias et al.[28] as a molecule that showed selectivity for the first bromodomain of BET proteins with a K_d of 3.4 μM. It possesses an alkylacetamide chain similar to K-ac, linked to a 2,3,4,5-tetrahydro-1*H*-pyrido[4,3-*b*]indol-1-one scaffold which interacts with residues that are unique to the first bromodomain of BRD4 (BRD4 BD1). Olinone was a suitable starting point for trying to recapitulate the acetamide binding motif in an NMP-containing analogue and we considered that either **4** or its homologue **12** would be suitable in creating this mimetic.

Following the reported procedure (Scheme 3),[28] 2,4-piperidinedione **13** was treated with phenylhydrazine **14** in ethanol to give the hydrazone intermediate **15**, which was then subjected to Fischer indole synthesis conditions, using 70% sulfuric acid to give the desired tricyclic scaffold **16**, albeit in modest yield. Alkylation of **16** with mesylates **4** and **12** using sodium bis(trimethylsilyl)amide as the base was low yielding, but both compounds **17** and **18** were successfully isolated. The difference in yields points to some hindrance due to the proximity of the NMP moiety in **4** towards **16**. ^{1}H NMR confirmed the selective alkylation at the indole nitrogen of the tricycle and not the lactam, with the disappearance of the indole NH proton resonance.

2.2. BRD4 BD1 FRET assay results

With this series of compounds in hand, the esters **2** and **10**, alcohols **3** and **11**, and Olinone analogues **17** and **18** were all evaluated as inhibitors of BRD4 BD1 binding to a tetra-acetylated histone peptide using a fluorescence resonance energy transfer (FRET)-based assay. The results of the assays are shown in Table 1.

The simple NMP analogues **2**, **3**, **10** and **11** showed comparable binding to NMP itself showing that 4-substitution was tolerated in the BRD4 BD1 binding site. The Olinone analogues **17** and **18** showed much improved affinity relative to NMP, consistent with the anticipated mimicry of the K-ac motif by the NMP functional group. Compound **17** was the higher affinity ligand with an IC_{50} of 24 μM, while compound **18** had an IC_{50} of 79 μM, marking an improvement of NMP's activity by 110-fold and 33-fold, respectively (dose response curves of **17** and **18** are available in Supplementary Fig. S1). Olinone is reported to have a K_d of 3.4 μM as measured by ITC, which we considered comparable to **17** given the differences in the assay formats.[28]

2.3. X-ray crystallography

We successfully obtained crystal structures of compounds **10**, **17** and **18** in complex with BRD4 BD1, which allowed us to assess the

Table 1
Preliminary SAR data on NMP derivatives.

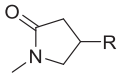

Compound Number	R =	IC_{50} (μM ± SEM)[a]	LE (kcal/mol NHA)[c]
	H	2660 ± 480	0.50
2		6880 ± 300	0.27
3		4110 ± 380	0.36
10		2120 ± 270	0.30
11		4810 ± 60	0.32
17	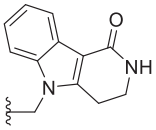	24 ± 2[b]	0.29
18	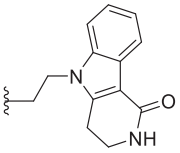	79 ± 3[b]	0.24

[a] Unless stated otherwise, all results of means are n ≥ 2.
[b] SD reported.
[c] Ligand efficiency = 1.37(−log(IC_{50})) / NHA. Control compound used: **I-BET726** (IC_{50}: 0.01 μM). NHA, non-hydrogen atom.

mimicry of K-ac in these compounds. As shown in Fig. 2, the NMP segment of **10** retains its mimicry of K-ac, interacting with Asn140 and Tyr97, while the ester interacts with the WPF shelf of BRD4 BD1. The WPF shelf is often targeted by selective inhibitors given its lack of conservation between bromodomains.[47] Here, the ester moiety interacts with residues Trp81 and Pro82 through weak vdW interactions.

The X-ray crystal structures of **17** and **18** show that, in both cases, the tricyclic scaffolds align with that of Olinone with a root mean square (RMS) for the heavy atoms of 0.56 Å and 0.24 Å, respectively. As anticipated, the NMP moiety of **17** and **18** mimics the acetamide group of Olinone and closely overlays with the reported structures of NMP (electron density maps can be found in Supplementary Fig. S2). While the pharmacophore elements of **17** and **18** are identical, the linkers differ in the conformation and stereochemical configuration at the NMP stereocentre. Despite each NMP derivative being submitted as a racemic mixture, density maps point to single enantiomers observed in the crystal form. Compound **17** is found in the same relative configuration as compound **10** and their backbones overlay closely (RMS = 0.36 Å). In contrast, compound **18** shows the opposite relative stereochemistry while accommodating an extended chain conformation (Fig. 3, Supplementary Video S2 and S3). Under the Cahn-Ingold-Prelog nomenclature, the absolute configuration is *R* for each of **10**, **17** and **18**.

3. Conclusion

In summary, we have demonstrated the use of NMP derivatives as fragments that can be used in the design of bromodomain ligands. We have successfully developed two synthetic schemes for six functionalised derivatives of NMP which can be produced on multigram scales. An X-ray crystal structure of one of these derivatives (**10**) in complex with BRD4 BD1 shows that it retains a similar mode of binding to that

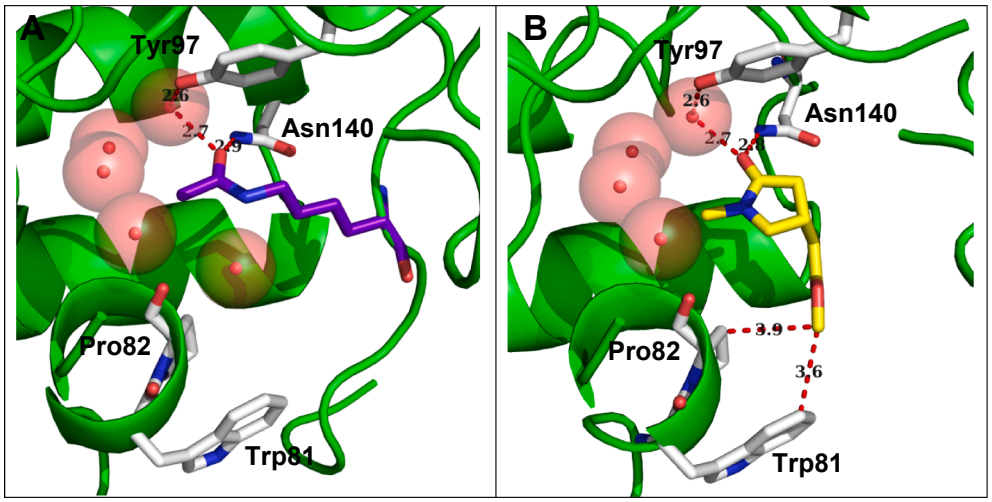

Figure 2. Comparison of binding substrates in the bromodomain binding site of BRD4 BD1. A. K-ac (purple blue, PDB: 3UVW). B. (*R*)-**10** (yellow, PDB: 6PRT, resolution: 1.3 Å). Water molecules shown as red spheres. Pro86, Val87 and Asp88 were hidden for better visualisation. Distances in Å, highlighted by red dashes. (For interpretation of the references to colour in this figure legend, the reader is referred to the web version of this article.)

previously observed for NMP.

The precursors **4** and **12** have been employed in the synthesis of two compounds, **17** and **18**, based on the inhibitor Olinone. The inhibition of bromodomain binding to an acetylated histone peptide by **17** and **18** is comparable to the parent compound and both compounds precisely mimic the parent compound in the BRD4 BD1 binding site.

These results should encourage the further exploration of NMP as a fragment in bromodomain inhibition for three reasons. Firstly, the pre-existing literature suggests that NMP is a general mimic of the acetamide function of K-ac. This suggests that the strategy applied here for BRD4 BD1 could be applied equally against one or more of the other 60 bromodomains in the epigenome. Secondly, the structures of **17** and **18** show that either of the stereochemical configurations of the NMP derivatives can be applied with success. Therefore, these are actually pairs of fragments which may be expected to have their own selectivity profiles. Further work to resolve or synthesise the individual stereoisomers is on-going. Finally, the variety of functionalities in the six fragments described here opens the door for alternate reactions to make products such as amines, ethers, amides and esters. Taken together, these results have further proved the usefulness of NMP as a mimetic fragment and the potential of its incorporation into other known inhibitors.

4. Experimental

4.1. Chemistry

^{1}H and ^{13}C Nuclear Magnetic Resonance spectra were conducted on a Bruker Advance III Nanobay 400 MHz spectrometer coupled to the BACS 60 automatic sample changer and obtained at 400.1 MHz and 100.6 MHz, respectively. All spectra were processed using MestReNova 6.0 software. The chemical shifts of all ^{1}H were measured relative to the expected solvent peaks of the respective NMR solvents; $CDCl_3$, 7.26; MeOD, 3.31. The chemical shifts of all ^{13}C were measured relative to the expected solvent peaks of the respective NMR solvents; $CDCl_3$, 77.2; MeOD, 49.0. The data for all spectra are reported in the following format: chemical shift (integration, multiplicity, coupling constant, assignment). Multiplicity is defined as; s = singlet, d = doublet, t = triplet, q = quartet, quint. = quintet, dd = doublet of doublets, td = triplet of doublets, qd = quartet of doublets, ddd = doublet of doublet of doublets, m = multiplet. Coupling constants are applied as J in Hertz (Hz). For ^{1}H and ^{13}C spectra, refer to Supplementary Fig. S3.

All HRMS analyses were obtained using an Agilent 6224 TOF LC/MS Mass Spectrometer coupled to an Agilent 1290 Infinity (Agilent, Palo Alto, CA). All data were acquired and reference mass corrected via a dual-spray electrospray ionisation (ESI) source. Each scan or data point on the Total Ion Chromatogram (TIC) is an average of 13,700 transients, producing a spectrum every second. Mass spectra were created by averaging the scans across each peak and background subtracted against the first 10 s of the TIC. Acquisition was performed using the Agilent Mass Hunter Data Acquisition software version B.05.00 Build 5.0.5042.2 and analysis was performed using Mass Hunter Qualitative Analysis version B.05.00 Build 5.0.519.13.

All LCMS analyses were carried out on an Agilent 6100 Series Single Quad LC/MS coupled with an Agilent 1200 Series HPLC, 1260 Infinity G1312B Binary pump, 1260 Infinity G1367E 1260 HiP ALS autosampler and 1290 Infinity G4212A 1290 DAD detector. The liquid chromatography conditions were: reverse phase HPLC analysis fitted with a Luna C8(2) 5 µL 50 × 4.6 mm 100 Å at a temperature of 30 °C. The sample injection volume was 5 µL, which was run in 0.1% formic acid in acetonitrile at a gradient of 5–100% over 10 min. Detection methods were either 254 nm or 214 nm. The mass spectrum conditions were: Quadrupole ion source with Multimode-ES. The drying gas temperature was 300 °C and the vaporizer temperature was 200 °C. The capillary voltage in positive mode was 2000 V, while in negative mode, the capillary voltage was 4000 V. The scan range was 100–1000 *m/z* with a step size of 0.1 s over 10 min.

TLCs were carried out on Merck TLC Silica gel 60 F_{254} plates using the appropriate mobile phase. Purification by column chromatography was conducted with Davisil Chromatographic Silica LC60A (40–63 µm) using the specified mobile phases.

Compound purity was determined using an Agilent 1260 Infinity Analytical HPLC (1260 Infinity G1322A Degasser, 1260 Infinity G1312B Binary pump, G1367E HiP ALS autosampler, 1260 Infinity G1316A Thermostatted Column Compartment, and 1260 Infinity G4212B DAD detector. The liquid chromatography conditions were: reverse phase HPLC analysis fitted with a Zorbax Eclipse Plus C18 Rapid Resolution 4.6 × 100 mm 3.5-Micron. The sample injection volume was 1 µL, which was run in Solvent A (0.1% TFA in H_2O) and Solvent B (0.1% TFA in CH_3CN), with a gradient of 5–100% Solvent B over a 10-minute period. All compounds submitted for assays and X-ray crystallography studies were assessed for purity of 95% or greater on 214 nm and 254 nm.

4.1.1. Methyl 1-methyl-5-oxo-3-pyrrolidine carboxylate (2)

40% Methylamine solution in H_2O (10 mL) was dissolved in methanol (125 mL) in an ice-bath and stirred. Dimethyl itaconate **1** (15.1 g, 94.8 mmol) dissolved in methanol (275 mL) was added dropwise to the stirring mixture. After an hour, the ice-bath was removed and the reaction continued to stir for a further 24 h. The mixture was concentrated under reduced pressure and the residue purified by vacuum distillation to afford **2** as an oil (13.7 g, 91%). **^{1}H NMR** (400 MHz,

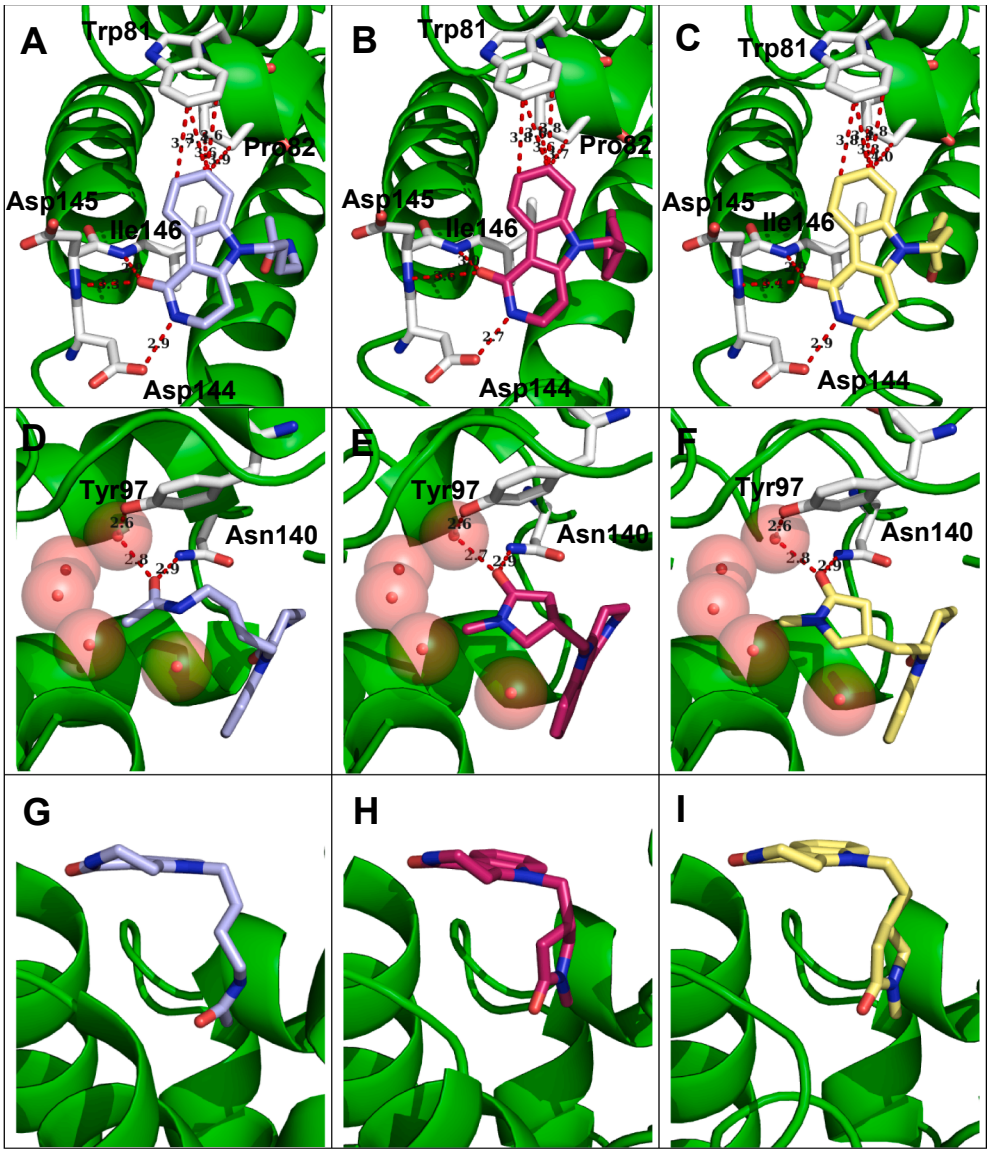

Figure 3. Comparison of Olinone and its respective analogues in BRD4 BD1. [A–C] 2,3,4,5-Tetrahydro-1*H*-pyrido[4,3-*b*]indol-1-one scaffold. [D–F] K-ac binding site. Water molecules shown as red spheres. Pro86, Val87 and Asp88 were hidden for better visualisation. Distances in Å, highlighted by red dashes. [G–I] Linker group visualisation. [A, D, G] Olinone (light blue, PDB: 4QB3). [B, E, H] (*R*)-**17** (warm pink, PDB: 6PS9, resolution: 1.59 Å). [C, F, I] (*R*)-**18** (pale yellow, PDB: 6PSB, resolution: 1.21 Å). (For interpretation of the references to colour in this figure legend, the reader is referred to the web version of this article.)

$CDCl_3$) δ 3.71 (s, 3H), 3.58 (ddd, J = 22.8, 14.4, 8.2 Hz, 2H), 3.27–3.16 (m, 1H), 2.82 (s, 3H), 2.73–2.57 (m, 2H) ppm. **^{13}C NMR** (101 MHz, $CDCl_3$) δ 173.4, 172.5, 52.6, 51.2, 35.9, 34.0, 29.6 ppm. **ESI-MS**, *m/z* 158.2 $[M+H]^+$; **HR-MS**: *m/z* calcd. for $C_7H_{11}NO_3$ $[M+H]^+$: 158.0812; found 158.0813; **HPLC** (PP gradient, MeOH): 3.27 min.

*4.1.2. 4-(Hydroxymethyl)-1-methylpyrrolidin-2-one (**3**)*

Methyl 1-methyl-5-oxo-3-pyrrolidine carboxylate **2** (10.5 g, 67.1 mmol) was dissolved in ethanol (400 mL) and stirred at room temperature. Sodium borohydride (25.3 g, 0.671 mol) was added slowly in small portions over a 7h period. After this period, water (20 mL) was added to form a cloudy mixture. The quenched mixture was then filtered through Celite 545 and carefully concentrated to a white solid by rotary evaporation. The solid was taken up in $CHCl_3$ (500 mL) and left to stir overnight. The mixture was dried with Na_2SO_4, filtered through filter paper and concentrated under reduced pressure to afford a crude oil. Purification by column chromatography (Mobile phase: 5% MeOH in $CHCl_3$) afforded **3** as a clear oil (6.82 g, 79%). **^{1}H NMR** (400 MHz, MeOD) δ 3.58–3.47 (m, 3H), 3.26 (dd, J = 10.1, 5.2 Hz, 1H), 2.61–2.44 (m, 2H), 2.19 (dd, J = 16.5, 5.4 Hz, 1H) ppm. **^{13}C NMR** (101 MHz, MeOD) δ 176.7, 64.9, 53.4, 34.77, 34.37, 29.8 ppm. **ESI-MS**, *m/z* 130.1 $[M+H]^+$. **HR-MS**: *m/z* calcd. for $C_6H_{10}NO_2$ $[M+H]^+$: 130.0863; found 130.0863; **HPLC** (PP gradient, MeOH): 1.75 min.

*4.1.3. (1-Methyl-5-oxopyrrolidin-3-yl)methyl methanesulfonate (**4**)*

In a 50 mL round-bottom flask, 4-(hydroxymethyl)-1-methylpyrrolidin-2-one **3** (209 mg, 1.62 mmol) was weighed out, then dissolved in CH_2Cl_2 (5 mL). The flask was placed in an ice bath, sealed with a rubber septum and purged with N_2. DIPEA (565 µL, 3.24 mmol) and MsCl (150 µL, 1.95 mmol) were added via syringe and the mixture was left to stir for 4 h. After this time, the mixture was quenched with water (20 mL) and the CH_2Cl_2 layer separated. The aqueous layer was washed with additional CH_2Cl_2 (3 × 20 mL). The organic layers were combined, dried with $MgSO_4$, filtered and concentrated via rotary evaporation to give the crude mesylate as a yellow oil. This oil was then purified using a silica column (Mobile phase: 2% MeOH in CH_2Cl_2) to give **4** as a clear oil (190 mg, 59%). **^{1}H NMR** (400 MHz, $CDCl_3$) δ 4.16 (qd, J = 10.0, 6.8 Hz, 2H), 3.51 (dd, J = 10.2, 8.2 Hz, 1H), 3.21 (dd, J = 10.2, 5.2 Hz, 1H), 3.01 (s, 3H), 2.85–2.73 (m, 4H), 2.53 (dd, J = 17.1, 9.4 Hz, 1H), 2.16 (dd, J = 17.1, 6.2 Hz, 1H) ppm. **^{13}C NMR** (101 MHz, $CDCl_3$) δ 172.8, 70.4, 51.4, 37.5, 33.3, 30.7, 29.6 ppm. **ESI-MS**, *m/z* 208.0 $[M+H]^+$; **HR-MS**: *m/z* calcd. for $C_7H_{13}NO_4S$ $[M+H]^+$: 207.0565; found 207.0567; **HPLC** (PP gradient, MeOH): 2.36 min.

4.1.4. Dimethyl 3-(nitromethyl)glutarate (6)

In a 250 mL round-bottom flask, nitromethane (14.9 mL, 0.352 mol) was added to dimethyl glutaconate **5** (5.56 g, 35.2 mmol). 1,1,3,3-Tetramethylguanidine (882 µL, 7.03 mmol) was added dropwise to the mixture. After complete addition, the mixture was left to stir overnight. The mixture was quenched with 5% HCl (75 mL), then washed with diethyl ether (3 × 75 mL). The organic layers were collected, combined and dried with $MgSO_4$. The solvent was filtered and evaporated under reduced pressure to give a brown-coloured oil. The resin was purified using silica gel chromatography (Mobile phase: 10% EtOAc in petroleum benzine, TLCs checked at 25% EtOAc in petroleum benzine) to afford **7** as a clear oil (3.32 g, 47%). **^{1}H NMR** (400 MHz, $CDCl_3$) δ 4.62 (d, J = 6.1 Hz, 2H), 3.71 (s, 6H), 3.13–3.00 (m, 1H), 2.56 (dd, J = 6.6, 1.1 Hz, 4H) ppm. **^{13}C NMR** (101 MHz, $CDCl_3$) δ 171.6, 77.5, 52.1, 35.1, 30.7 ppm.

4.1.5. Methyl 2-(5-oxopyrrolidin-3-yl)acetate (8)

In a 250 mL three-neck round-bottom flask purged with N_2, 10% Pd/C (332 mg) was added and submerged in CH_2Cl_2. Dimethyl 3-(nitromethyl)glutarate **6** (3.32 g, 15.2 mmol) was dissolved in acetic acid (150 mL) and added to the flask, then stirring began. The flask was then flushed with N_2 three times, followed by H_2 three times. Progress was monitored using NMR and LCMS. Once the starting material and hydroxylamine intermediate were consumed, the flask was purged with N_2 and the Pd/C was filtered through glass microfiber filter paper. The solvent was then evaporated off to give the amine **7** as a caramel-coloured oil. The amine was then dissolved in MeOH (75 mL), basified with Et_3N (1 mL) and heated under reflux. The solvent and base were evaporated off under reduced pressure to give the crude lactam **8** as a yellow resin. The resin was purified by column chromatography (Mobile phase: 2% MeOH in CH_2Cl_2) to afford **8** as a white solid (1.61 g, 68%). **^{1}H NMR** (400 MHz, $CDCl_3$) δ 7.07 (br s, 1H), 3.62 (s, 3H), 3.54 (dd, J = 9.9, 7.8 Hz, 1H), 3.02 (dd, J = 9.9, 6.2 Hz, 1H), 2.86–2.75 (m, 1H), 2.52–2.40 (m, 3H), 1.99 (dd, J = 16.9, 7.3 Hz, 1H) ppm. **^{13}C NMR** (101 MHz, $CDCl_3$) δ 177.7, 171.8, 51.3, 47.4, 38.0, 36.2, 30.6 ppm. **ESI-MS**: m/z 158.1 $[M+H]^+$.

4.1.6. Methyl 2-(1-methyl-5-oxopyrrolidin-3-yl)acetate (10)

To a solution of lactam **8** (1.12 g, 7.09 mmol) in acetone (120 mL) was added paraformaldehyde (1.07 g, 35.5 mmol) and K_2CO_3 (132 mg), followed by the addition of water (13 mL). The mixture was then sonicated for 4 h at 20-minute intervals with 10-minute rests. The mixture was then filtered and the filtrate was concentrated under reduced pressure to give the crude hemiaminal **9** as an opaque oil. The oil was purified by silica column chromatography (Mobile phase: 5% MeOH in CH_2Cl_2) to give **9** as a clear oil. The hemiaminal **9** was then dissolved in $CHCl_3$ (125 mL), to which CF_3COOH (25 mL) and Et_3SiH (25 mL) were added, and the mixture was stirred at room temperature overnight. The mixture was then quenched with water (75 mL) and the organic layer was separated. The aqueous layer was washed with additional $CHCl_3$ (2 × 75 mL). The organic layers were combined, dried with $MgSO_4$, filtered and concentrated under reduced pressure to afford a biphasic oil. This was purified by column chromatography (neat EtOAc), giving **10** as a clear oil (1.08 g, 89%). **^{1}H NMR** (400 MHz, $CDCl_3$) δ 3.67 (s, 3H), 3.57 (dd, J = 10.0, 7.9 Hz, 1H), 3.06 (dd, J = 10.0, 6.0 Hz, 1H), 2.85–2.68 (m, 4H), 2.58 (dd, J = 16.8, 9.0 Hz, 1H), 2.53–2.38 (m, 2H), 2.08 (dd, J = 16.8, 7.0 Hz, 1H) ppm. **^{13}C NMR** (101 MHz, $CDCl_3$) δ 173.7, 172.2, 54.8, 51.9, 38.8, 37.1, 29.6, 27.9 ppm. **ESI-MS**: m/z 172.1 $[M+H]^+$ **HR-MS**: m/z calc. for $C_8H_{13}NO_3$ $[M+H]^+$: 171.0895; found 171.0899. **HPLC** (PP gradient, MeOH): 3.31 min.

4.1.7. 4-(2-Hydroxyethyl)-1-methylpyrrolidin-2-one (11)

In a 100 mL round-bottom flask, methyl 2-(1-methyl-5-oxopyrrolidin-3-yl)acetate **10** (446 mg, 2.61 mmol) was dissolved in EtOH (25 mL). $NaBH_4$ (0.99 g, 26.1 mmol) was then added over a period of 4 h, and the mixture was left to stir overnight. After completion, the mixture was quenched with water and the solvent was evaporated off under reduced pressure to give a white solid. The solid was then purified by column chromatography (Mobile phase: 5% MeOH in CH_2Cl_2) to obtain **11** as a clear oil (313 mg, 84%). **^{1}H NMR** (400 MHz, $CDCl_3$) δ 3.72–3.58 (m, 2H), 3.49 (dd, J = 9.7, 8.1 Hz, 1H), 3.07 (dd, J = 9.7, 6.7 Hz, 1H), 2.80 (s, 3H), 2.58–2.25 (m, 3H), 2.13–2.01 (m, 1H), 1.76–1.61 (m, 2H) ppm. **^{13}C NMR** (101 MHz, $CDCl_3$) δ 174.7, 60.7, 55.5, 37.51, 37.49, 29.68, 28.79 ppm. **ESI-MS**: m/z 222.0 $[M+H]^+$. **HR-MS**: m/z calc. for $C_7H_{13}NO_2$ $[M+H]^+$: 143.0946; found 143.0951. **HPLC** (PP gradient, MeOH): 2.09 min.

4.1.8. 2-(1-Methyl-5-oxopyrrolidin-3-yl)ethyl methanesulfonate (12)

In a 50 mL round-bottom flask, 4-(2-hydroxyethyl)-1-methylpyrrolidin-2-one **11** (128 mg, 0.893 mmol) was weighed out, then dissolved in CH_2Cl_2 (10 mL). The flask was placed in an ice bath, sealed with a rubber septum and purged with N_2. DIPEA (233 µL, 1.34 mmol) and MsCl (103 µL, 1.34 mmol) were added via syringe and the mixture was left to stir for 4 h. After this time, the mixture was quenched with water (20 mL) and the CH_2Cl_2 layer separated. The aqueous layer was washed with additional CH_2Cl_2 (3 × 20 mL). The organic layers were combined, dried with $MgSO_4$, filtered and concentrated via rotary evaporation to give the crude mesylate **12** as a yellow oil. This oil was then purified using silica gel chromatography (Mobile phase: 2% MeOH in CH_2Cl_2) to give **12** as a clear oil (122 mg, 62%). **^{1}H NMR** (400 MHz, $CDCl_3$) δ 4.31–4.18 (m, 2H), 3.53 (dd, J = 9.7, 8.0 Hz, 1H), 3.07 (dd, J = 9.7, 6.6 Hz, 1H), 3.01 (s, 3H), 2.82 (s, 3H), 2.61–2.47 (m, 2H), 2.14–2.03 (m, 1H), 1.94–1.86 (m, 2H) ppm. **^{13}C NMR** (101 MHz, $CDCl_3$) δ 173.7, 67.7, 54.8, 37.60, 37.13, 34.1, 29.67, 28.60 ppm. **ESI-MS**: m/z 222.0 $[M+H]^+$. **HR-MS**: m/z calc. for $C_8H_{15}NO_4S$ $[M+H]^+$: 221.0726; found 221.0726. **HPLC** (PP gradient, MeOH): 3.28 min.

4.1.9. 2,3,4,5-Tetrahydro-1H-pyrido[4,3-b]indol-1-one (16)

2,4-Piperidinedione **13** (500 mg, 4.42 mmol) was weighed into a 100 mL round-bottom flask, and phenylhydrazine **14** (434 µL, 4.42 mmol) was added. The mixture was dissolved in EtOH (50 mL) and stirred at reflux overnight. The solvent was evaporated off to give the hydrazone **15** as a crimson oil. This was cooled to 0 °C, dissolved in 70% sulfuric acid (20 mL) and stirred for 4 h. The acid was neutralised with 2 M NaOH and the aqueous layer was washed with EtOAc (3 × 50 mL). The organic layers were combined, dried with $MgSO_4$, filtered and concentrated under reduced pressure to afford a yellow/brown resin. This was purified with silica gel chromatography (Mobile phase: Gradient of 3–5% MeOH in CH_2Cl_2) to acquire **16** as a yellow resin (137 mg, 17%). **^{1}H NMR** (400 MHz, $CDCl_3$) δ 8.91 (br s, 1H), 8.17–8.09 (m, 1H), 7.38–7.31 (m, 1H), 7.25–7.17 (m, 2H), 5.53 (br s, 1H), 3.63 (t, J = 6.9 Hz, 2H), 3.02 (t, J = 6.9 Hz, 2H) ppm. **ESI-MS**: m/z 187.1 $[M+H]^+$. **HPLC** (PP gradient, MeOH): 4.36 min.

4.1.10. 5-((1-Methyl-5-oxopyrrolidin-3-yl)methyl)-2,3,4,5-tetrahydro-1H-pyrido[4,3-b]indol-1-one (17)

In a 25 mL round-bottom flask, 2,3,4,5-tetrahydro-1*H*-pyrido[4,3-*b*]indol-1-one **16** (36.5 mg, 0.196 mmol) was dissolved in DMF (3 mL). The flask was sealed, purged with N_2 and then chilled to −78 °C. NaHMDS (94 µL, 0.294 mmol, 1 M in THF) was added via syringe and the mixture was stirred for 30 min. After this time, 2-(1-methyl-5-oxopyrrolidin-3-yl)ethyl methanesulfonate **12** (60.9 mg, 0.294 mmol) was weighed, dissolved in DMF (1 mL) and added via syringe. The mixture was warmed to room temperature, then heated to 90 °C and left stirring overnight. After this time, the mixture was quenched with a saturated aqueous solution of $NaHCO_3$ (40 mL) and washed with EtOAc (3 × 40 mL). The combined organic layer were dried with $MgSO_4$, filtered and concentrated under reduced pressure to obtain a yellow oil. The oil was purified using a silica column (Mobile phase: 5% MeOH in CH_2Cl_2) to obtain **17** as a yellow oil (3.80 mg, 6%). **^{1}H NMR** (400 MHz, $CDCl_3$) δ 8.23–8.18 (m, 1H), 7.33–7.26 (m, 3H), 5.53 (br s, 1H), 4.14 (d, J = 8.0 Hz, 2H), 3.70 (t, J = 6.9 Hz, 2H), 3.38 (dd, J = 10.2, 7.2 Hz,

1H), 3.12–2.92 (m, 4H), 2.85 (s, 3H), 2.57 (dd, J = 17.1, 8.3 Hz, 1H), 2.18 (dd, J = 16.9, 4.8 Hz, 1H) ppm. **^{13}C NMR** (101 MHz, $CDCl_3$) δ 123.13, 122.58, 121.62, 109.4, 52.2, 46.7, 40.8, 35.2, 32.2, 29.9, 22.5 ppm. **ESI-MS**: m/z 297.9 $[M+H]^+$. **HR-MS**: m/z calc. for $C_{17}H_{19}N_3O_2$ $[M+H]^+$: 297.1477; found 297.1475. **HPLC** (PP gradient, MeOH): 4.32 min.

4.1.11. 5-(2-(1-Methyl-5-oxopyrrolidin-3-yl)ethyl)-2,3,4,5-tetrahydro-1H-pyrido[4,3-b]indol-1-one (18)

In a 50 mL round-bottom flask, 2,3,4,5-tetrahydro-1*H*-pyrido[4,3-*b*] indol-1-one **16** (45 mg, 0.241 mmol) was dissolved in DMF (3 mL). The flask was sealed, purged with N_2 and then chilled to –78 °C. NaHMDS (362 µL, 0.362 mmol, 1 M in THF) was added via syringe and the mixture was stirred for 30 min. After this time, 2-(1-methyl-5-oxopyrrolidin-3-yl)ethyl methanesulfonate **12** (80 mg, 0.362 mmol) dissolved in DMF (1 mL) was added via syringe. The mixture was warmed to room temperature, then heated to 90 °C and left stirring overnight. After this time, the mixture was quenched with a saturated aqueous solution of $NaHCO_3$ (40 mL) and washed with EtOAc (3 × 40 mL). The combined organic layers were dried with $MgSO_4$, filtered and concentrated under reduced pressure to obtain a yellow oil. The oil was purified with a silica column (Mobile phase: Gradient of 2–7% MeOH in CH_2Cl_2) to obtain **18** as a yellow oil (24.7 mg, 33%). **^{1}H NMR** (400 MHz, $CDCl_3$) δ 8.24–8.18 (m, 1H), 7.33–7.24 (m, 3H), 5.68 (br s, 1H), 4.21–4.05 (m, 2H), 3.69 (td, J = 6.8, 1.9 Hz, 2H), 3.46 (dd, J = 9.7, 8.1 Hz, 1H), 3.05–2.97 (m, 3H), 2.82 (s, 3H), 2.59 (dd, J = 16.5, 8.9 Hz, 1H), 2.42–2.28 (m, 1H), 2.14 (dd, J = 16.5, 7.2 Hz, 1H), 2.07–1.86 (m, 2H) ppm. **^{13}C NMR** (101 MHz, $CDCl_3$) δ 173.5, 166.9, 143.8, 136.5, 125.7, 122.72, 122.17, 121.44, 109.2, 106.2, 55.1, 42.0, 40.7, 37.2, 35.1, 29.7, 29.2, 22.2 ppm. **ESI-MS**: m/z 312.0 $[M+H]^+$. **HR-MS**: m/z calc. for $C_{18}H_{21}N_3O_2$ $[M+H]^+$: 311.1634; found 311.1641. **HPLC** (PP gradient, MeOH): 4.644 min.

4.2. Fluorescence resonance energy transfer assay

The IC_{50}s were measured using a Fluorescence Resonance Energy Transfer (FRET) assay. The assay is dependent on a europium (Eu^{3+}) cryptate-conjugated antibody/glutathione *S*-transferase (GST) fused to BRD4 BD1 (49–170) complex binding to a Streptavidin-D2 biotinylated, tetra-acetylated histone H4 peptide, SGRG-K(Ac)-GG-K(Ac)-GLG-K(Ac)-GGAK(Ac)-RHRKVGG-K-(Biotin) complex. Both Streptavidin-D2 and the Eu^{3+} cryptate-conjugated antibody were purchased from CisBio Assays. When both are in close proximity, a 337 nm laser light activates the Eu^{3+} donor which emits at 620 nm, resulting in D2 fluorescence at 665 nm. The assays were performed in 384-well volume microtiter plates. The serially diluted small molecule inhibitors were diluted in 10% (v/v) DMSO resulting in a final concentration of 1% DMSO in each well. The final reagent concentrations in each well were 10 nM of GST-BRD4 BD1 protein, 40 nM of histone H4 peptide, 5 nM of Eu^{3+} cryptate-conjugated GST-antibody, 6.25 nM Streptavidin-D2 in 50 mM Hepes, 50 mM NaCl, 0.5 mM CHAPS, 400 mM KF, 0.01% (w/v) BSA, pH 7.5. After mixing and incubation at room temperature for at least 1.5 h, the plates were measured in a PheraStar plate reader (BMG Labtech) (excitation: 337 nm; emission: 620 and 665 nm). The binding activity was expressed as the ratio of fluorescence at 665 nm divided by that at 620 nm corrected by the ratio determined in the absence of binding. Using the GraphPad program, binding was plotted against inhibitor concentration followed by non-linear regression to determine the IC_{50}.

4.3. Protein expression and purification

BRD4 BD1 was expressed in *E. coli* using induction by addition of 1 mM isopropyl β-D-1-thiogalactopyranoside at 24 °C for 16 h. The bacteria were lysed in 50 mM Hepes pH 7.5, 300 mM NaCl, 5 mM imidazole, 5% (v/v) glycerol using a combination of lysozyme treatment (1 mg/mL of lysate and incubated on ice for 30 min) and sonication. The His-tagged BRD4 BD1 was purified using Ni-agarose chromatography with elution in 50 mM Hepes pH 7.5, 300 mM NaCl, 500 mM imidazole, 5% (v/v) glycerol. The 6-His tag was then removed by TEV protease digestion. The bromodomain was further purified using gel filtration chromatography using a Superdex-75, 16/60 column (GE Healthcare) in a buffer containing 50 mM Hepes pH 7.5, 0.3 M NaCl and 5% glycerol.

4.4. Crystallisation and data collection

X-ray crystal structures were obtained using a 6-His tagged bromodomain. The concentrated BRD4 BD1 protein (17 mg/mL, stored at −80 °C) was then incubated with 5 mM ligand at 4 °C for 16 h. Crystals were obtained using the hanging drop method in 24-well plates using 1 µL drops of protein and the reservoir solution containing 0.2 M $NaNO_3$, PEG-3350 (35%) and ethylene glycol (6% v/v) concentrations. The crystals were cryoprotected using mother liquor supplemented with 5 mM ligand and then were flash frozen in liquid nitrogen. All datasets were collected at the Australian Synchrotron, part of ANSTO, on the MX1 and MX2 beamlines.[48–50] The datasets were processed with either automated data processing pipeline implemented at the beamlines, using *xdsme*[51] and *AIMLESS*,[52] or manually using *iMOSFLM*[53] and *AIMLESS*[52] from the CCP4 suite.[54] 5% of reflections in each dataset were flagged for calculation of R_{free}. A summary of statistics is provided in Supplementary Table S1. Molecular replacement was performed with *Phaser*[55] using a previously solved structure of BRD4 as a search model (PDB: 5DW2). The final structures were obtained after several rounds of manual refinement using *Coot*[56] and refinement with *phenix.refine*.[57]

Declaration of Competing Interest

The authors declare no conflicts of interest.

Acknowledgements

This work was supported by a Research Training Program scholarship from the Monash Institute of Pharmaceutical Sciences, NHMRC project, program and fellowship grants, and a Cancer Council Victoria Venture Grant. This research was undertaken in part using the MX2 beamline at the Australian Synchrotron, part of ANSTO, and the Australian Cancer Research Foundation (ACRF) detector. Initial crystallisation screens were carried out at the CSIRO Collaborative Crystallisation Centre (www.csiro.au/C3) in Melbourne, Australia.

Appendix A. Supplementary material

Supplementary data to this article can be found online at https://doi.org/10.1016/j.bmc.2019.115157.

References

1. Huang B, Yang XD, Zhou MM, Ozato K, Chen LF. Brd4 coactivates transcriptional activation of NF-kappaB via specific binding to acetylated RelA. *Mol Cell Biol.* 2009;29:1375–1387.
2. Ciro M, Prosperini E, Quarto M, et al. ATAD2 is a novel cofactor for MYC, overexpressed and amplified in aggressive tumors. *Cancer Res.* 2009;69:8491–8498.
3. French CA, Miyoshi I, Kubonishi I, Grier HE, Perez-Atayde AR, Fletcher JA. BRD4-NUT fusion oncogene: a novel mechanism in aggressive carcinoma. *Cancer Res.* 2003;63:304–307.
4. Zou JX, Guo L, Revenko AS, et al. Androgen-induced coactivator ANCCA mediates specific androgen receptor signaling in prostate cancer. *Cancer Res.* 2009;69:3339–3346.
5. Mujtaba S, He Y, Zeng L, et al. Structural basis of lysine-acetylated HIV-1 Tat recognition by PCAF bromodomain. *Mol Cell.* 2002;9:575–586.
6. Cardenas-Mora J, Spindler JE, Jang MK, McBride AA. Dimerization of the papillomavirus E2 protein is required for efficient mitotic chromosome association and Brd4 binding. *J Virol.* 2008;82:7298–7305.
7. Lin A, Wang S, Nguyen T, Shire K, Frappier L. The EBNA1 protein of Epstein-Barr virus functionally interacts with Brd4. *J Virol.* 2008;82:12009–12019.
8. Lu P, Shen Y, Yang H, et al. BET inhibitors RVX-208 and PFI-1 reactivate HIV-1 from

latency. *Sci Rep.* 2017;7:16646.
9. Darcis G, Kula A, Bouchat S, et al. An in-depth comparison of latency-reversing agent combinations in various in vitro and ex vivo HIV-1 latency models identified bryostatin-1 + JQ1 and ingenol-B + JQ1 to potently reactivate viral gene expression. *PLoS Pathog.* 2015;11:e1005063.
10. Das A, Chai JC, Yang CS, et al. Dual transcriptome sequencing reveals resistance of TLR4 ligand-activated bone marrow-derived macrophages to inflammation mediated by the BET inhibitor JQ1. *Sci Rep.* 2015;5:16932.
11. Nicodeme E, Jeffrey KL, Schaefer U, et al. Suppression of inflammation by a synthetic histone mimic. *Nature.* 2010;468:1119–1123.
12. Anand P, Brown JD, Lin CY, et al. BET bromodomains mediate transcriptional pause release in heart failure. *Cell.* 2013;154:569–582.
13. Gilham D, Wasiak S, Tsujikawa LM, et al. RVX-208, a BET-inhibitor for treating atherosclerotic cardiovascular disease, raises ApoA-I/HDL and represses pathways that contribute to cardiovascular disease. *Atherosclerosis.* 2016;247:48–57.
14. Crawford TD, Audia JE, Bellon S, et al. GNE-886: a potent and selective inhibitor of the cat eye syndrome chromosome region candidate 2 bromodomain (CECR2). *ACS Med Chem Lett.* 2017;8:737–741.
15. Igoe N, Bayle ED, Fedorov O, et al. Design of a biased potent small molecule inhibitor of the bromodomain and PHD finger-containing (BRPF) proteins suitable for cellular and in vivo studies. *J Med Chem.* 2017;60:668–680.
16. Picaud S, Fedorov O, Thanasopoulou A, et al. Generation of a selective small molecule inhibitor of the CBP/p300 bromodomain for leukemia therapy. *Cancer Res.* 2015;75:5106–5119.
17. Siebel AL, Trinh SK, Formosa MF, et al. Effects of the BET-inhibitor, RVX-208 on the HDL lipidome and glucose metabolism in individuals with prediabetes: a randomized controlled trial. *Metabolism.* 2016;65:904–914.
18. Stathis A, Zucca E, Bekradda M, et al. Clinical response of carcinomas harboring the BRD4-NUT oncoprotein to the targeted bromodomain inhibitor OTX015/MK-8628. *Cancer Discov.* 2016;6:492–500.
19. Siu KT, Ramachandran J, Yee AJ, et al. Preclinical activity of CPI-0610, a novel small-molecule bromodomain and extra-terminal protein inhibitor in the therapy of multiple myeloma. *Leukemia.* 2017;31:1760–1769.
20. Mirguet O, Gosmini R, Toum J, et al. Discovery of epigenetic regulator I-BET762: lead optimization to afford a clinical candidate inhibitor of the BET bromodomains. *J Med Chem.* 2013;56:7501–7515.
21. Shortt J, Ott CJ, Johnstone RW, Bradner JE. A chemical probe toolbox for dissecting the cancer epigenome. *Nat Rev Cancer.* 2017;17:160.
22. Dhalluin C, Carlson JE, Zeng L, He C, Aggarwal AK, Zhou MM. Structure and ligand of a histone acetyltransferase bromodomain. *Nature.* 1999;399:491–496.
23. Filippakopoulos P, Qi J, Picaud S, et al. Selective inhibition of BET bromodomains. *Nature.* 2010;468:1067–1073.
24. Chung CW, Dean AW, Woolven JM, Bamborough P. Fragment-based discovery of bromodomain inhibitors part 1: inhibitor binding modes and implications for lead discovery. *J Med Chem.* 2012;55:576–586.
25. Bamborough P, Diallo H, Goodacre JD, et al. Fragment-based discovery of bromodomain inhibitors part 2: optimization of phenylisoxazole sulfonamides. *J Med Chem.* 2012;55:587–596.
26. Hewings DS, Wang M, Philpott M, et al. 3,5-dimethylisoxazoles act as acetyl-lysine-mimetic bromodomain ligands. *J Med Chem.* 2011;54:6761–6770.
27. Vidler LR, Filippakopoulos P, Fedorov O, et al. Discovery of novel small-molecule inhibitors of BRD4 using structure-based virtual screening. *J Med Chem.* 2013;56:8073–8088.
28. Gacias M, Gerona-Navarro G, Plotnikov AN, et al. Selective chemical modulation of gene transcription favors oligodendrocyte lineage progression. *Chem Biol.* 2014;21:841–854.
29. Ozer HG, El-Gamal D, Powell B, et al. BRD4 profiling identifies critical chronic lymphocytic leukemia oncogenic circuits and reveals sensitivity to PLX51107, a novel structurally distinct BET inhibitor. *Cancer Discov.* 2018;8:458–477.
30. Dawson MA, Prinjha RK, Dittmann A, et al. Inhibition of BET recruitment to chromatin as an effective treatment for MLL-fusion leukaemia. *Nature.* 2011;478:529–533.
31. Philpott M, Yang J, Tumber T, et al. Bromodomain-peptide displacement assays for interactome mapping and inhibitor discovery. *Mol Biosyst.* 2011;7:2899–2908.
32. Shortt J, Hsu AK, Martin BP, et al. The drug vehicle and solvent N-methylpyrrolidone is an immunomodulator and antimyeloma compound. *Cell Rep.* 2014;7:1009–1019.
33. NMP in Relapsed Refractory Myeloma. https://ClinicalTrials.gov/show/NCT02468687.
34. Ghayor C, Correro RM, Lange K, Karfeld-Sulzer LS, Gratz KW, Weber FE. Inhibition of osteoclast differentiation and bone resorption by N-methylpyrrolidone. *J Biol Chem.* 2011;286:24458–24466.
35. Ghayor C, Gjoksi B, Siegenthaler B, Weber FE. N-methyl pyrrolidone (NMP) inhibits lipopolysaccharide-induced inflammation by suppressing NF-kappaB signaling. *Inflamm Res.* 2015;64:527–536.
36. Gjoksi B, Ghayor C, Bhattacharya I, Zenobi-Wong M, Weber FE. The bromodomain inhibitor N-methyl pyrrolidone reduced fat accumulation in an ovariectomized rat model. *Clin Epigenet.* 2016;8:42.
37. Rooney TP, Filippakopoulos P, Fedorov O, et al. A series of potent CREBBP bromodomain ligands reveals an induced-fit pocket stabilized by a cation-pi interaction. *Angew Chem Int Ed Engl.* 2014;53:6126–6130.
38. Zoretic PA, Barcelos F, Jardin J, Bhakta C. Synthetic Approaches to 10-Azaprostaglandins. *J Org Chem.* 1980;45:810–814.
39. Stanetty P, Turner M, Mihovilovic MD. Synthesis of pyrrolo[2,3-d][1,2,3]thiadiazole-6-carboxylates via the Hurd-Mori reaction. Investigating the effect of the N-protecting group on the cyclization. *Molecules.* 2005;10:367–375.
40. Hanessian S, Buckle R, Bayrakdarian M. Design and synthesis of a novel class of constrained tricyclic pyrrolizidinone carboxylic acids as carbapenem mimics. *J Org Chem.* 2002;67:3387–3397.
41. Kobayashi S, Kobayashi K, Hirai K. Trials for the synthesis of (R)-4-mercapto-pyrrolidin-2-one ((R)-MPD). *Synlett.* 1999;1999:909–912.
42. Felluga F, Gombac V, Pitacco G, Valentin E. A convenient chemoenzymatic synthesis of (R)-(−) and (S)-(+)-homo-β-proline. *Tetrahedron Asymmetry.* 2004;15:3323–3327.
43. Wang L, Dong M, Lowary TL. Synthesis of unusual N-acylated aminosugar fragments of Mycobacterium marinum lipooligosaccharide IV. *J Org Chem.* 2015;80:2767–2780.
44. Kwak H-S, Koo KD, Lim D, et al. *Preparation of 5-oxopyrrolidine-2-carboxamide and 2-oxoimidazolidine-4-carboxamide derivatives as beta-secretase inhibitors.* S. Korea: LG Life Sciences, Ltd.; 2009:108.
45. Ma S, Han X, Krishnan S, Virgil SC, Stoltz BM. Catalytic enantioselective stereoablative alkylation of 3-halooxindoles: facile access to oxindoles with C3 all-carbon quaternary stereocenters. *Angew Chem Int Ed Engl.* 2009;48:8037–8041.
46. Bennett SNL, Goldberg FW, Leach A, Whittamore PRO, Soerme P. *Preparation of adamantyl iminocarbonyl-substituted pyrimidines as inhibitors of 11βHSD1.* Swed: AstraZeneca AB; 2011:40.
47. Romero FA, Taylor AM, Crawford TD, Tsui V, Cote A, Magnuson S. Disrupting acetyllysine recognition: progress in the development of bromodomain inhibitors. *J Med Chem.* 2016;59:1271–1298.
48. McPhillips TM, McPhillips SE, Chiu HJ, et al. Blu-Ice and the Distributed Control System: software for data acquisition and instrument control at macromolecular crystallography beamlines. *J Synchrotron Radiat.* 2002;9:401–406.
49. Cowieson NP, Aragao D, Clift M, et al. MX1: a bending-magnet crystallography beamline serving both chemical and macromolecular crystallography communities at the Australian Synchrotron. *J Synchrotron Radiat.* 2015;22:187–190.
50. Aragao D, Aishima J, Cherukuvada H, et al. MX2: a high-flux undulator microfocus beamline serving both the chemical and macromolecular crystallography communities at the Australian Synchrotron. *J Synchrotron Radiat.* 2018;25:885–891.
51. Kabsch W. Integration, scaling, space-group assignment and post-refinement. *Acta Crystallogr D Biol Crystallogr.* 2010;66:133–144.
52. Evans PR, Murshudov GN. How good are my data and what is the resolution? *Acta Crystallogr D Biol Crystallogr.* 2013;69:1204–1214.
53. Battye TG, Kontogiannis L, Johnson O, Powell HR, Leslie AG. iMOSFLM: a new graphical interface for diffraction-image processing with MOSFLM. *Acta Crystallogr D Biol Crystallogr.* 2011;67:271–281.
54. Winn MD, Ballard CC, Cowtan KD, et al. Overview of the CCP4 suite and current developments. *Acta Crystallogr D Biol Crystallogr.* 2011;67:235–242.
55. McCoy AJ, Grosse-Kunstleve RW, Adams PD, Winn MD, Storoni LC, Read RJ. Phaser crystallographic software. *J Appl Crystallogr.* 2007;40:658–674.
56. Emsley P, Lohkamp B, Scott WG, Cowtan K. Features and development of Coot. *Acta Crystallogr D Biol Crystallogr.* 2010;66:486–501.
57. Afonine PV, Grosse-Kunstleve RW, Echols N, et al. Towards automated crystallographic structure refinement with phenix.refine. *Acta Crystallogr D Biol Crystallogr.* 2012;68:352–367.